Contents lists available at ScienceDirect

Materials and Design

journal homepage: www.elsevier.com

Early adhesion of cells to ferromagnetic shape memory alloys functionalized with plasma assembled biomolecules – A single force spectroscopy study

Mehmet Volkan Cakir[a], Uta Allenstein[a, b, c], Mareike Zink[a, *], Stefan G. Mayr[b, c]

[a] *Soft Matter Physics Division and Junior Research Group Biotechnology and Biomedicine, Peter Debye Institute for Soft Matter Physics, Leipzig University, Linnéstr. 5, 04103 Leipzig, Germany*
[b] *Leibniz Institute of Surface Engineering (IOM) e.V., Permoser Str. 15, 04318 Leipzig, Germany*
[c] *Division of Surface Physics, Department of Physics and Earth Sciences, Leipzig University, Leipzig, Germany*

ARTICLE INFO

Article history:
Received 22 May 2018
Received in revised form 3 August 2018
Accepted 4 August 2018
Available online xxx

Keywords:
Single cell force spectroscopy
Cell adhesion
Ferromagnetic shape memory alloys
Fe-Pd
Lysine

ABSTRACT

Biomaterial performance and integration of prostheses in vivo strongly depend on the ability of cells to adhere. Plasma-assisted functionalization of smart metals with biopolymers, including plasma polymerized L-lysine (PPLL), constitutes a recently-developed promising approach to synthesize highly flexible, yet robust and strongly adherent protein coatings that support cell-biomaterial interaction. In the present study we employ single cell force spectroscopy to demonstrate that PPLL coatings promote early adhesion of fibroblast cells on the ferromagnetic shape memory alloy Fe—Pd – a promising magnetically switchable biomaterial. By varying the contact time of a cell with the substrate surface, we show that the forces and work needed to fully detach a cell increase with time and quantify bioactivity of the material. In contrast to glass and PPLL-coated glass, cell detachment from Fe—Pd requires much larger work, while a PPLL biofunctionalization further improves cell adhesion and binding affinity by an increased detachment work on short time scales. Together with a time-dependent bond model we postulate a transition from unspecific to specific cell adhesion on Fe—Pd and PPLL-coated Fe—Pd, while on glass detachment forces are lower and level off to a saturation regime on short times prior to the expected time necessary for specific integrin-based bond formation.

1. Introduction

Cell adhesion to the extracellular matrix (ECM) or any other scaffold is a prerequisite for survival, proliferation and many other cellular processes. However, at a tissue-implant interface ECM molecules that support specific cell adhesion are lacking, particularly when composed of metals employed e.g. for joint replacements [1]. Bioactive coatings can enhance biomaterial performance and cell attachment [2], while alternatively cells deposit ECM molecules themselves to which they then bind [3]. The first adhesion event between the cell and a biomaterial results in the formation of focal complexes and can be mediated by hyaluronic acid, which occurs on time scales of seconds [4]. After this first soft-binding step, maturation to focal adhesion takes place that strong and specific adhesion sites form via the interaction of adhesion receptors with ECM molecules [5,6].

Within the last decade more and more artificial materials have arisen for biomedical and biotechnological applications. In contact with living cells, tissues and organs, new challenges have come up regarding the material - cell interface and coupling of the biomaterial to the implant. The use of biomaterials include high-end applications such as organ replacement [7], tissue engineering [8,9], dental [10], orthopedic [11] and cochlear implants [12], as well as cardiovascular [13], diagnostic [14] and pharmaceutical applications [15]. New approaches aim to design biomaterials which are not solely replacing damaged tissue by a passive implant that interfere with the surrounding tissue as little as possible, but active implants that interact with desirable stimuli [16,17]. Nevertheless, functioning of medical devices and implants relies on good integration and cellular adhesion in vivo. However, many widely used implant materials naturally do not promote adequate cell adhesion for the integration of the implant, and weak mechanical coupling, e.g. for bone prosthesis, can result in tissue degeneration and implant loosening due to stress shielding [18]. One difficulty is that the elastic moduli of widely used implant materials composed of metals have elastic moduli decades larger than that of tissues. Moreover, proteins that support cell adhesion such as fibronectin hardly adsorb on stainless steel and titanium dioxide surfaces [19,20]. Coatings that promote adhesion, such as hydroxyapatite for improved bone attachment, are frequently brittle and can rupture from the underlying implant.

Ferromagnetic shape memory alloys, including Fe—Pd, constitute an example of an upcoming smart materials class with promising properties for biomedical applications [21]. Inducing high reversible strains at moderate stresses in contact with tissues opens up the possibility of applying magnetic fields even long after insertion of the implants for readjustment, while this alloy also comprises the superelastic effect of conventional shape memory materials [22]. Basic bio-

* Corresponding author.
Email address: zink@physik.uni-leipzig.de (M. Zink)

https://doi.org/10.1016/j.matdes.2018.08.012
0264-1275/

compatibility of the Fe—Pd alloy with murine fibroblast cells, primary human osteoblast cells and human mammary epithelial cells has previously been investigated using immunofluorescence methods [22,23]. Additionally, cell adhesion promoting biomolecules such as fibronectin and laminin enhance cell attachment even more [22,24]. In fact, Allenstein et al. showed that plasma polymerized L-lysine (PPLL) adsorbs and strongly binds to the Fe-site of the alloy in contrast to conventional poly-L-lysine coatings resulting in improved cell adhesion and spreading [25]. PPLL is a flexible, yet ultra-durable coating which demonstrates plasma-assisted functionalization a new approach to couple proteins to a metal surface. Nevertheless, even for uncoated Fe—Pd the number of focal contacts of adherent cells is higher compared to titanium and glass substrates; however, a quantitative analysis of the acting adhesion forces is lacking [26].

Most studies addressing the interaction of cells with implant materials only focus on cell spreading behavior and the number of focal contacts that form during cell adhesion, while a quantitative analysis of adhesion forces and work needed to detach the cells is not employed. In this study we quantify early adhesion forces of murine fibroblast cells on Fe—Pd thin films, as well as samples coated with PPLL by using AFM-based single cell force spectroscopy (SCFS) initially described by Benoit et al. [27]. Results were compared with cell adhesion on pure glass and PPLL coated glass surfaces. During each SCFS cycle, immobilized cells attached to a cantilever are pushed to the substrate with a defined force and retracted again after a certain contact time. The respective detachment forces and the employed work are monitored to quantify cell-surface interaction for the different materials as a measure for bioactivity of the surface independent of the type of cell-surface binding, viz. specific and unspecific bonds. Moreover, a time-dependent bond formation model between cells and substrates is employed to analyze the detachment forces and work obtained from measurements with different contact times. Our results demonstrate that early adhesion forces and the work necessary to detach cells is much larger for Fe—Pd and PPLL coated Fe—Pd compared to glass and PPLL-coated glass which quantifies good bioactivity of this ferromagnetic shape memory alloy and makes it a promising candidate for medical applications.

2. Materials and methods

2.1. Fe-Pd film preparation and biofunctionalization

50 nm thick polycrystalline $Fe_{70}Pd_{30}$ films were sputter deposited onto soda lime glass substrates from a $Fe_{70}Pd_{30}$ alloy target (ACI Alloys, San Jose, CA); a film thickness as low as this guaranteed optical transparency, while already revealing a fully closed surface under the chosen deposition conditions. The procedure was carried out in a chamber that was evacuated and flooded with an argon flow of 3.5 sccm which provides a sputtering pressure of 5×10^{-3} mbar. Argon plasma was excited by an RF input power of 45 W. We would like to point out that previous in vitro assessments on vapor-deposited as well as sputtered single- and polycrystalline $Fe_{70}Pd_{30}$ thin films and roughness graded polycrystalline splats of the same stoichiometry revealed excellent biocompatibility and even bioactivity in contact with different cell types including NIH 3t3 fibroblasts [22,28].

Plasma polymerized L-lysine coating was employed as described previously [25]. Briefly, L-lysine monomer powder (Sigma-Aldrich, CAS No. L5501) that is diluted to a concentration of 0.009 mol/l via pure ethanol (Merck KGaA, CAS No. 64-17-5) was injected into a pulsed plasma inside a quartz tube of 3 cm inner diameter with a flow rate of 0.24 ml/min. The previously evacuated quartz tube is flooded with 200 sccm argon flow that introduces 10 mbar argon pressure. Excitation of the plasma is carried out inductively by a 13.56 MHz RF-supply attached to a self-constructed matching network. Plasma is stabilized at an input power of 15 W pulsing with 80 Hz and 8% duty cycle before adding the L-lysine solution. However, parameters are changed to 10 W and 2% duty cycle during the deposition. Films achieve a thickness of 50 nm after around 60 min. Flow of plasma and lysine is turned off after deposition while argon atmosphere is kept for additional 5 min. After the procedure residual lysine monomers that failed to cross-link to the coating are removed by rinsing with deionized water. In the following, plasma polymerized L-lysine coated Fe—Pd samples are referred to as FePd + Lysine.

Control experiments were performed on pure glass substrates and plasma polymerized L-lysine coated glass (glass + Lysine).

2.2. Cells and culturing procedures

We employed NIH/3T3 embryonic mouse fibroblast cells since they have been widely used to study the biocompatibility and bioactivity of many materials including the ferromagnetic shape memory alloy Fe—Pd [22,24,26]. Cells are incubated at 37 °C in 5% CO_2 humidified atmosphere in full growth medium of Dulbecco's Modified Eagles Medium (DMEM) (Biochrom, Cat. No. F0435) complemented with 10% Calf Serum (CS) (PAA, Cat. No. B15-004) and 1% Penicillin - Streptomycin antibiotic solution (PS) (Sigma-Aldrich, Cat. No. P0781). Single cell force spectroscopy measurements were carried out in pure DMEM to avoid the presence of adhesion influencing serum proteins.

2.3. Single cell force spectroscopy and cantilevers

For single cell force spectroscopy (SCFS) measurements a JPK CellHesion® 200 (JPK Instruments AG, Berlin) scanning force microscope is used which allows a cantilever deflection in z-direction of 100 µm. The CellHesion® 200 is equipped on a Zeiss phase contrast microscope. Tipless cantilevers (NanoWorld, Arrow TL2, NanoWorld AG, Switzerland) are used with spring constants around 30 mN m^{-1}.

2.4. Cantilever functionalization and cell attachment

In our study, a cell is attached to a tipless cantilever prior to SCFS measurements. To this end, the cantilever apex is functionalized using a fibronectin coating which allows strong specific adhesion of the cell to the cantilever surface. Cantilever coating solution (6 µl fibronectin and 44 µl phosphate buffered saline (PBS) per cantilever) is mixed and added to the cantilever. After incubating for 2 h at 37 °C, coated cantilevers are rinsed with PBS.

To capture and attach a single cell to the fibronectin-coated cantilever, a suspension of cells is added to a medium-filled culture dish. The cantilever is positioned above a single cell and pushed down onto the cell with a force of 0.5 nN for 10 s. Then the cantilever is retracted with the attached cell. After a waiting time of 30–45 min, in which the probing cell can firmly attach to the cantilever, the SCFS measurements were performed.

2.5. Cell-substrate adhesion measurement cycle

In one SCFS measurement cycle, the cell on the cantilever is pushed onto the substrate (Fe—Pd, FePd + Lysine, glass and glass + Lysine, respectively) and retracted after a certain contact time. During retraction the attachment force between cell and substrate is measured as pulling force on the cantilever. Each captured single cell

is measured for five different contact times (5 s, 10 s, 20 s, 40 s, and 80 s, respectively) in a row. The same set of measurements for five different contact times is also repeated five times for each captured single cell on different positions over the substrate.

Acquired force-distance (FD) curves are corrected using baseline and offset correction by the provided data management software of the setup (sources of abnormalities in SCFS measurements and correction methods are reviewed in Ref. [29]).

2.6. Data procession and statistical analysis

The maximum detachment force F_{max} and work of detachment W_{detach} were obtained from force distance (FD) curves. Processing and analysis of FD curves were carried out by the CellHesion 200 software (JPK Instruments, Germany).

We carried out experiments on 4 glass, 4 PPLL coated glass, 5 Fe—Pd and 4 PPLL coated Fe—Pd samples using fresh cells for each. For each cell on the cantilever, we recorded 5 force distance curves for 5 contact times (25 FD curves in total) on different locations on the sample surface. In total, we gained 425 FD curves for four different contact times and four different substrate materials.

The distribution parameters (median, 1st and 3rd quartiles) are used to quantify and compare cell-substrate interactions on different materials. In fact, we employed median values instead of mean values for the data distribution of each contact time due to the stochastic nature of the determined adhesion process (see Discussion) which are not necessarily perfect normal distributions. In this case median values are a more robust and reliable measure against outliers and skewed distributions compared to mean values to describe the central tendency of distributions of each contact time.

3. Results

3.1. Force-distance behavior between cell and substrates

During each SCFS measurement a force-distance (FD) curve between the cantilever distance from the substrate and the acting force is acquired as shown in Fig. 1. Here four regimes are visible: (1) approaching to the surface with the cell attached to the cantilever, (2) getting into contact with the surface until a preset contact force is reached, (3) retracting the cantilever after a certain contact time and (4) moving away from the surface until the cell detaches from the surface (Fig. 1). When the cell is pressed onto the substrate, cell-surface adhesion points form, which sequentially break during retraction and thus leave behind a unique and complex signature curve. Contact times between cells and substrates of 5 s up to 80 s are employed.

In our study the largest adhesion force in the FD curve (F_{max}) represents the maximum strength of cell–substrate binding before the cell starts to detach. After F_{max} is reached, the force decreases rapidly while the number of bonds between cell and substrate decreases and the applied force, which is held constant at 1 nN, is shared between less and less bonds. W_{detach} is the work of detachment and is obtained from the area under the FD curve during retraction (Fig. 1) by integrating over the measured force as a function of cantilever distance. We would like to point out that F_{max} and W_{detach} can result from unspecific bonds, e.g. via electrostatic interaction, as well as specific bonds such as integrin-mediated interaction, or both binding types.

3.2. Forces during single cell detachment

The maximum detachment forces F_{max} for NIH/3 t3 fibroblasts on Fe—Pd and plasma polymerized L-lysine (PPLL) coated samples, as

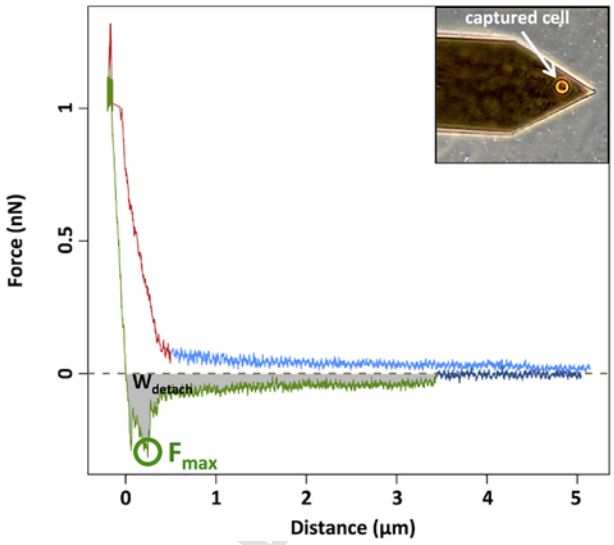

Fig. 1. Force-distance (FD) curve of a SCFS measurement in which a fibroblast cell attached to a cantilever is pressed against a PPLL-coated Fe—Pd (denoted as FePd + Lysine) surface for 10 s. Subsequently, the cantilever with the cell is retracted. There are four basic regimes of the FD curve representing the cantilever approach to the surface (light blue), getting into contact (red), retracting (and consequently detaching) (green) and moving away from surface (dark blue). F_{max} represents the maximum pulling force value that is reached during retraction before detachment occurs and W_{detach} represents the work as the area under the retraction curve. The inset figure shows the cantilever with a just captured cell. (For interpretation of the references to color in this figure legend, the reader is referred to the web version of this article.)

well as control measurements with glass and PPLL-coated glass are shown in Fig. 2 for different contact times.

It becomes evident that the maximum detachment force increases with contact time for all substrate materials, while the maximum attained force values are larger for glass and PPLL coated glass compared to Fe—Pd and PPLL-coated Fe—Pd. However largest median F_{max} values are seen for Fe—Pd substrates for the shortest contact

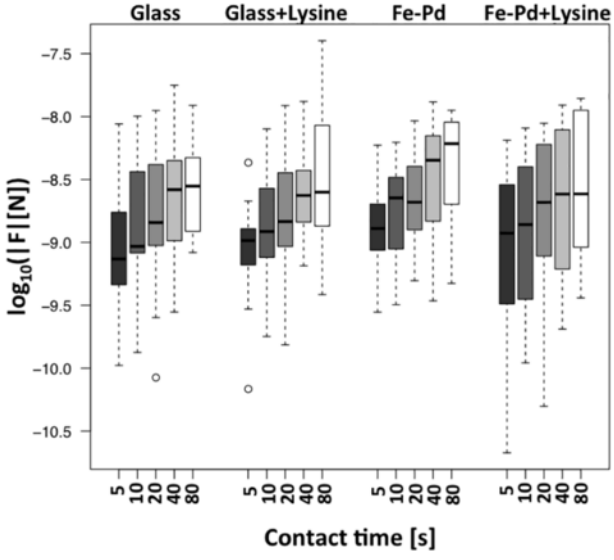

Fig. 2. Maximum detachment force distributions for different contact times of a fibroblast cell with four different surfaces (logarithmic scale is used to present differences more clearly). Central lines represent medians, hinges represent 1st and 3rd quartiles, notches represent 95% confidence intervals of medians, whiskers represent hinges ± 1.5IQR (Interquartile Range) while single points represent outliers.

time of 5 s (1.3 nN for Fe—Pd vs. 0.7 nN for glass), as well as for the longest contact time of 80 s (6.1 nN for Fe—Pd vs. 2.8 nN for glass) (median values in Figs. 2 and 3). To analyze our observation of increased detachment forces for longer contact times in more detail, we employed a time dependent bond model proposed by P. Elter et al. [30] Here the adhesion strength A is described as a function of the form

$$A = C_1\left(1 - e^{(-C_2 t)}\right) \tag{1}$$

with the contact time t. C_1 defines a plateau height in units of a force and C_2 represents a time constant that defines the slope of the curve with the unit of inverse time. $\lim_{t\to\infty} A = C_1$ can be understood as the measure of maximum adhesion force that can be achieved between a cell and a certain substrate. Thus, the adhesion strength is always lower than C_1 and reaches a maximum value of C_1 only for long contact times.

Within the time-dependent bond model, a certain point on the curve describing the adhesion strength can be expressed by

$$\sigma C_1 = C_1\left[1 - e^{(-C_2\tau(\sigma))}\right] \tag{2}$$

with $0<\sigma\leq 1$ being a proportionality constant between the adhesion strength for the achieved force after a certain contact time and C_1. Thus, the time that is needed to reach a proportion of the maximum value (the maximum value that can be reached according to the employed model), $\tau(\sigma)$ is given by

$$\tau(\sigma) = -\frac{\ln(1-\sigma)}{C_2} \tag{3}$$

It can be seen that C_2 alters the curvature of the curve that defines $\tau(\sigma)$. For instance, the time needed to reach 95% of the maximum ($\sigma = 0.95$) is

$$\tau_{0.95} = -\frac{\ln(0.05)}{C_2} \tag{4}$$

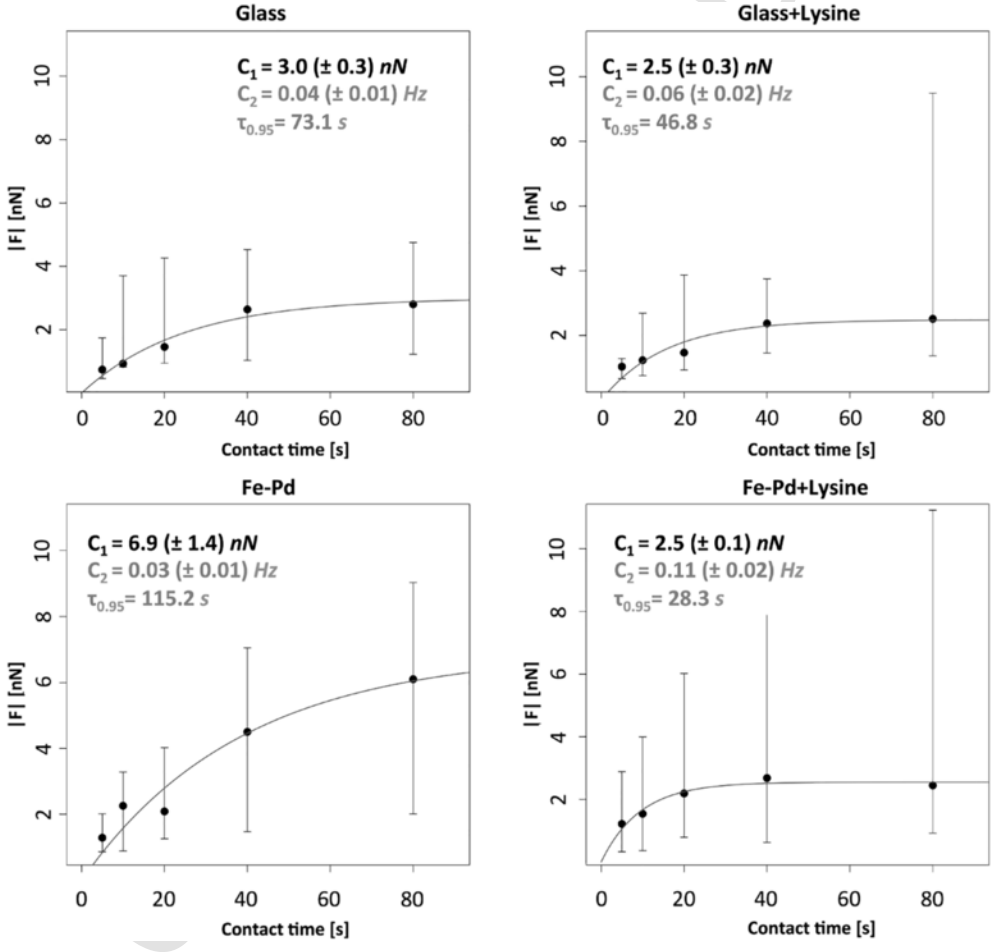

Fig. 3. Time-dependent adhesion bond model (solid curve) for median values of detachment forces for different contact times (points). The fits correspond to the time-dependent bond model (Eq. (1)) with the model parameters C_1, C_2 and $\tau_{0.95}$.

The application of Eq. (1) to our obtained maximum detachment forces F_{max} – which correspond to the adhesion strengths from the time dependent bond model – for increasing contact times is shown in Fig. 3. From the obtained parameters C_1 and $\tau_{0.95}$ we get the maximum attainable force and the time needed to reach 95% of this force.

According to the employed time dependent bond model cells on Fe—Pd can attain a substantially higher maximum force value ($C_1 = 6.9 \pm 1.4$ nN) compared to other substrates, which is twice as high as the second greatest C_1 value found on glass (3.0 ± 0.3 nN) (Fig. 3). With plasma polymerized lysine coatings, the maximum forces for Fe—Pd and glass are similar and around 2.5 nN. However, cells on FePd+Lysine substrates reach the maximum force much faster than on glass and glass+Lysine substrates as shown by the $\tau_{0.95}$ values in Fig. 3.

Interestingly, plasma polymerized L-lysine coatings, which previously have been shown to enhance cell adhesion on Fe—Pd [25], do not increase the maximum force with which cells bind to the surface. However, maximum detachment forces and detachment works are not related directly, as the former strongly depend on the nature of detachment, viz. covering the whole range from instantaneous to sequential; F_{max} thus cannot be interpreted as a measure of entire cell-surface interaction.

3.3. Work during cell detachment

The detachment work needed to fully separate a cell from the substrate surface, is shown in Fig. 4 for all employed materials. Here the work W_{detach} represents the sum of all rupture events via breakage of all binding sites (specific or unspecific bonds or both) to the substrate and therefore reflects the overall cell adhesion.

A general observation from Fig. 4 is that W_{detach} increases with increasing contact time as expected. The median values for the distributions obtained for Fe—Pd and FePd+Lysine are increasing with contact times, while for glass+Lysine the detachment work saturates after 20 s contact time. Only for pure glass samples a continuous increase is not observed and the median detachment work is slightly reduced from 2.3 fJ at 40 s contact time to 1.6 fJ after 80 s (median values in Figs. 4 and 5). The largest median detachment work is seen after 80 s for FePd+Lysine with 5.4 fJ (Figs. 4 and 5). On average the detachment work for different contact times is generally larger on pure Fe—Pd than on glass and glass+Lysine, while largest values are found for PPLL-coated Fe—Pd.

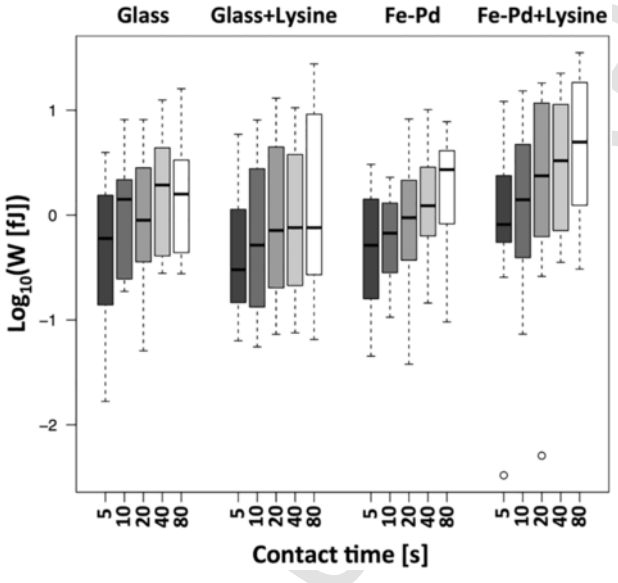

Fig. 4. Work of detachment value distributions as function of contact time for fibroblast interaction with glass and Fe—Pd including plasma-polymerized L-lysine coatings in logarithmic scale. Central lines represent medians, hinges represent 1st and 3rd quartiles, whiskers represent hinges ± 1.5IQR (Interquartile Range) while single points represent outliers.

We also applied the adhesion bond model to the median values of W_{detach} (Fig. 5) in which here *A* corresponds to the detachment work as a function of contact time and C_1 to the saturation work for long times. Thus, from the maximum work to separate the cell from the surface, it becomes evident that Fe—Pd and FePd+Lysine outperform glass and glass+Lysine substrates by generating much higher binding strengths, probably by the formation of an increased number of bonds. Interestingly glass+Lysine substrates exhibit a smaller maximum work of detachment than pure glass.

$\tau_{0.95}$ is the time needed to reach 95% of the maximum detachment work. For glass and glass+Lysine $\tau_{0.95}$ values around 30 s were found, while for FePd+Lysine a saturation time of 142 s is determined. Thus, as seen from Fig. 5, for Fe—Pd the detachment work does not saturate and the model curve shows a much larger slope at 80 s contact time compared to all other materials. In summary, from the obtained detachment work values it becomes evident that much larger work is needed to detach cells from Fe—Pd and PPLL coated Fe—Pd compared to pure and coated glass surfaces. Moreover, PPLL promotes entire cell adhesion even better than Fe—Pd since for FePd+Lysine the largest detachment work for long contact times is found with a C_1 value of (6.5 ± 0.9) fJ.

4. Discussion

Even though cell adhesion is a prerequisite for cell proliferation and migration, as well as the performance of many implant materials, which must be integrated in the human body by strong binding to the surrounding tissue, it is still difficult to quantitatively assess the interaction of cells with a biomaterial. Cell adhesion is mainly investigated by detaching single cells or cell populations from a surface. For single cell detachment optical and magnetic tweezers [31–33], as well as micropipette aspiration [34] can be employed, while for cell populations mainly centrifugation techniques [35], spinning disks [36] and flow chambers [37] are applied (for an overview see Ref. [38]). Sobral et al. demonstrated an accelerated buoyancy adhesion assay in combination with morphometric analysis of adherent osteoblast cells on microgrooved surfaces [39]. With this technique it is possible to correlate cell spreading effects with adhesion forces. However, when quantifying the interaction of a cell with different biomaterials, it is important that the detachment forces and works are related to identical cell areas that are probed. Since the detachment work is the summation of energy of all rupture events, it is directly connected to the number of bonds formed between the cell and the substrate and therefore a direct measure of the bioactivity of the surface – independent of the type of cell-substrate binding. Thus, we employ a single cell force spectroscopy technique (for SCFS details see Ref. [27, 40, 41]) to quantify cell adhesion forces in terms of forces necessary to detach a cell in contact with a substrate and the corresponding detachment work. Here we cannot determine the contact area of a cell pressed against the substrates. However, since always the same cell type is employed with identical protocols, we expect that the cell-surface contact area is similar in all experiments. Moreover, the contact time of the cell to the investigated substrate is too short for cell spreading. Thus, an increase in the detachment work due to an increase in the

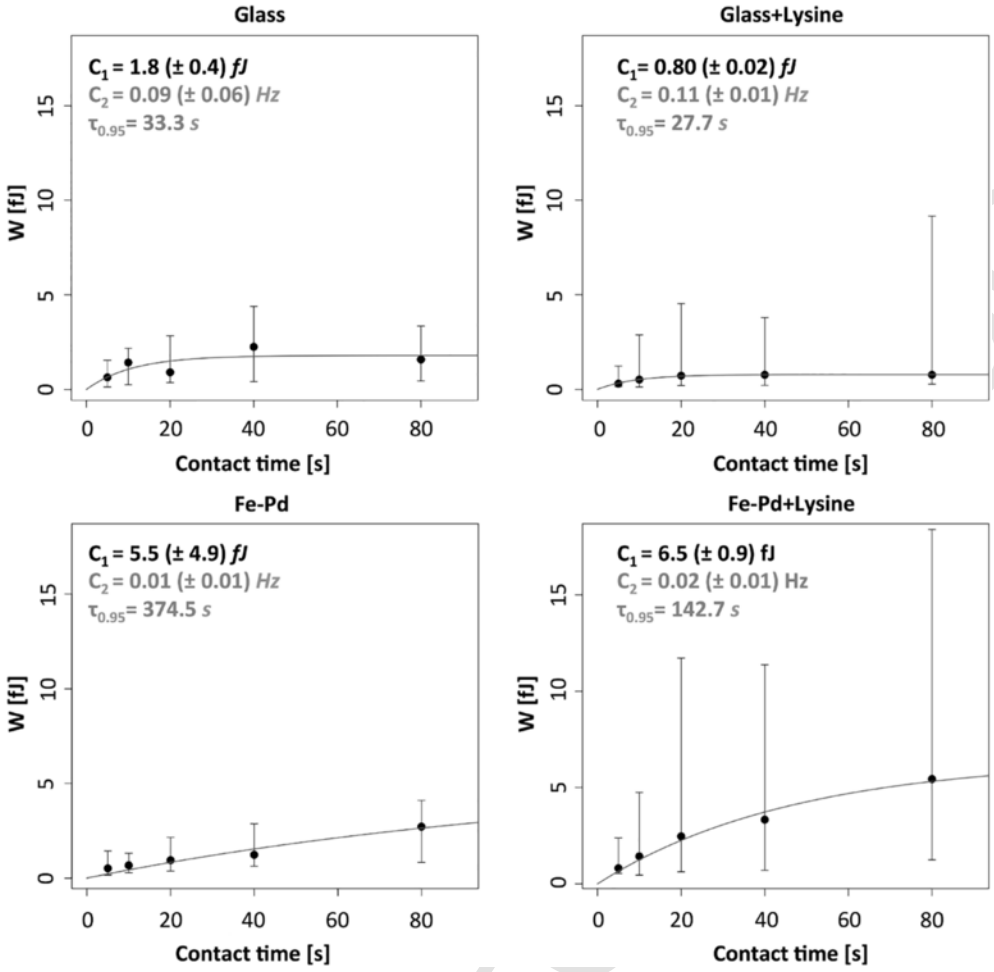

Fig. 5. Median values (points) of the detachment work as function of contact time (solid curve) for different substrate materials. The fits correspond to the time-dependent bond model (Eq. (1)) with the model parameters C_1, C_2 and $\tau_{0.95}$.

number of bonds for increasing cell areas during spreading is neglected.

In our study we investigated cell-substrate interaction of NIH/3T3 fibroblast cells with four different materials: (1) the ferromagnetic shape memory alloy Fe—Pd, (2) plasma polymerized L-lysine (PPLL) coated Fe—Pd, (3) glass cover slips and (4) PPLL coated glass. As recently shown, PPLL is a novel bioactive coating that supports cell adhesion and unspecific binding of cells [25]. Our SCFS data are compared with a time-dependent bond formation model which does not take the type of adhesion – specific or unspecific cell-substrate binding – into account and only describes the evolution of detachment forces and work. However, these parameters are a quantitative measure of a material's bioactivity on short time scales.

Before cell-surface interaction sites mature into focal adhesions, dot-like nascent adhesions and focal complexes form on time scales of tens of seconds, thus time scales employed in our SCFS measurements [4,42–45]. However, such binding events can only occur if ECM molecules that can bind to integrin receptors on the cell surface are present on the substrate surface. Due to the short contact time, expression and deposition of ECM molecules such as fibronectin from the cell to the substrate is not expected. Nevertheless, adherent cells continuously produce fibronectin [46]. In fact, preliminary data on fibroblast adhesion to titanium substrates show, that 30 min after cell seeding fibronectin is already expressed and 60 min after seeding enough fibronectin is already deposited on the cell surface that the formation of specific adhesion contacts via integrin receptors are observed [47]. Therefore, the employed 45 min waiting time for the cell to adhere to the cantilever is expected to be sufficient for fibronectin to be produced and transported to the cell surface which can then interact with the biomaterial during SCFS measurements and results in specific binding events between the cell and the substrate surface.

Besides the described specific binding events, unspecific binding are further expected to be present since PPLL interacts with fibroblast cells via electrostatic forces [25]. Thus, even without a direct evaluation of binding sites, we propose that from the calculated saturation times and the increased detachment forces and works, that unspecific and specific bonds form between the cell and the substrates which both contribute to a good bioactivity of the material.

It must be noted that the maximum detachment force may ether be limited by the interaction of (a) an ECM molecule with the cell or (b) binding of the molecule to the substrate. This could also explain why on glass smaller detachment forces are seen compared to Fe—Pd. Our previous study showed that already physisorbed RGD molecules bind much stronger to Fe—Pd surfaces compared to glass [24] and the "weak link" in cell-surface interaction is the binding of the molecule to the substrate, not to the cell. Due to prevalence of covalent bonds, this will be even more valid for PPLL functionalization. Thus, we expect that PPLL only weakly binds to glass that cells peel off the

coating during retraction of the cell – as similarly found before for cell spreading on RGD-coated glass [24] – resulting in a smaller detachment work for PPLL-coated glass compared to pure glass substrates. This observation is also in line with our determined saturation times, which show that on glass and PPLL-coated glass the maximum detachment forces occur on time scales below 73 s, thus likely before specific adhesion sites could be formed. Even though specific bonds form, rupture might occur on the surface-ECM molecule site and not on the molecule-cell interaction. To this end, we attribute differences in cell adhesion not to variations of the molecular structure of PPLL and poly-L-lysine varying upon different materials, but to differences in interaction strength of the functionalization to the underlying substrate – in line with previous studies [24,25].

However, it is questionable why the saturation time for a maximum detachment force on PPLL-coated Fe—Pd already occurs after 28 s. Most likely specific adhesions need longer contact times that were not reached in our experiments and the determined detachment forces result from unspecific binding sites. Comparison with saturation times of the maximum detachment work also shows that for PPLL-coated Fe—Pd the maximum number of binding sites for the employed contact area (which results from saturation of the detachment work) is not reached within the maximum contact time of 80 s, showing that more bonds are still forming. However, it is difficult to identify rupture events of specific bonds from the FD curve which are supposed to occur as "jumps". Counting the number of these events is not reliable since they overlap with rupture and bond-breaking events of other specific and unspecific binding sites. Nevertheless, from a qualitative analysis of the FD curves it could be assumed that the number of "jumps" increases with contact time. Thus, in contrast to glass and PPLL-coated glass, Fe—Pd and PPLL-coated Fe—Pd promote cell adhesion and most likely the formation of specific, integrin-mediated bonds since also the saturation times for the maximum detachment work is exceeding the times needed for early adhesion formation such as focal complexes.

Our obtained values of detachment forces and works are similar to SCFS studies of fibroblast adhesion on various materials including titanium, glass, and silicon including fibronectin coatings [30,48–51]. Elter et al. investigated the effect of fibronectin on fibroblast adhesion to silicon substrates. For a contact time of 10 s the mean maximum adhesion force was measured to be around 1 nN similar to our detachment forces, while the mean adhesion energy (viz. the detachment work) was around 3.8 fJ [48]. In our study the detachment work is found to be lower (around 1 fJ), while the C_1 parameter, which describes the saturation work for longer times, varies between 0.7 fJ and 6.5 fJ for the different substrate materials. These values are comparable to the force distribution and C_1 parameters reported by Elter et al. for early adhesion of fibroblasts on titanium substrates [30]. To this end, we conclude that PPLL on Fe—Pd supports early fibroblast adhesion much better than planar titanium surfaces and to a similar extent as a fibronectin coating.

Aliuos et al. reported a maximum detachment force of fibroblasts on glass of approximately 1 nN for 30 s contact time [49], similar to reports by Wittenburg et al. [51] and in line with our values around 1.5 nN for 20 s contact time. Interestingly, the reported detachment works exhibit a much wider distribution and, e.g. for fibroblast detachment from differently treated glass surfaces values below 5 fJ up to >13 fJ are described [51]. Thus, the number of early bonds, which is represented by the detachment work, drastically depends on the material and contact time. Nevertheless, we would like to point out that the adhesion receptors are distributed randomly on the cell surface [52] and the formation of bonds and adhesion clusters can be described as a stochastic process [53]. To this end, broader work distributions can be expected. Additionally, cell membrane fluctuations of the order of a few nanometers influence cell adhesion as well which make bond formation a statistical process [54]. Thus, when a cell comes into contact with the substrate, formation of binding sites is not an instantaneous process but occurs when cell receptors and ligands match. Thus, over time more and more bonds form which assemble into complexes. Due to the statistical nature of such processes wider force and work distributions and larger error bars can be expected as seen in our measurements.

It can be expected that for longer contact times of several minutes up to hours, the time-dependent bond model is not valid anymore. The parameter C_1 describes the saturation force or work. However, as seen for contact times of 30 min, detachment forces and works are up to three orders of magnitude larger compared to contact times of tens of seconds as reported by Weber et al. [55,56]. Thus, during maturation of focal complexes to focal adhesions on time scales of several tens of minutes, much stronger interaction sites area formed which would result in a further increase of the detachment force and work after the saturation regime in the time-dependent bond model. Additionally, spreading of cells and an increased projected cell area also contribute to enhanced adhesion in terms of increased detachment work.

In summary, our SCFS study on early cell adhesion clearly reveals Fe—Pd as a bioactive material that promotes fast cell attachment to the surface. We expect that both unspecific and specific binding – such as the assembly of focal complexes – contribute to the observed adhesion events. Moreover, a PPLL coating further improves cell attachment. Future studies will address a detailed evaluation of cell-surface interactions with respect to a detailed evaluation of the specific bond formation via integrin receptors, as well as the impact of short term adhesion on maturation of adhesion sites and adhesion strength on longer time scales of several hours.

5. Conclusion

SCFS is a powerful tool to quantify early cell adhesion in terms of forces and work necessary to detach cells from a surface on short time scales. Here we demonstrated that these data give evidence of strongly enhanced bioactivity of the ferromagnetic shape memory alloy Fe—Pd when plasma-functionalized with lysine coating compared to cells on plain Fe—Pd, as well as glass substrates and PPLL coated glass as reference. This behavior is not only attributed to an improved binding of cells to the PPLL coating, but also to the strong interaction of PPLL to the Fe-site of the underlying Fe—Pd substrate that directly results from plasma processing, while adhesion of PPLL coating to glass is evidently much weaker which can result in peel-off during cell retraction. Moreover, we conclude that enhanced early adhesion correlates with formation of strong contact sites such as focal adhesions on longer terms since previous studies clearly showed that Fe—Pd and especially with PPLL coating are bioactive substrates that promote cell spreading and adhesion on longer times. In fact, after a few days cells are much larger with an increased contact area and exhibit more focal adhesion sites compared to cells on glass substrates [25].

Since the type of cell-surface interaction is important for a better understanding of the bioactive properties of a biomaterial, future studies will focus on a detailed evaluation of cellular binding site formation such as specific contacts via immunohistochemistry. Moreover, the effect of the molecular structure and morphology of the underlying biofunctionalization on the maturation of focal complexes to focal adhesions will be addressed to investigate the molecular origin of the bioactive properties of the PPLL coating.

Author contribution

MVC and UA performed the experiments and analyzed the data; MZ, SGM and MVC wrote the manuscript; MZ and SGM designed the research and supervised the study; all authors discussed the results and commended on the manuscript.

Acknowledgments

We acknowledge J. Schulze for help with PPLL synthesis and N. John for help with Fe—Pd film deposition. T. Thalheim and S. Pawlizak are acknowledged for introducing the CellHesion technique and T. Müller, JPK AG for technical support. This work was funded in part by the German Science Foundation (DFG), Project "BIOSTRAIN", as well as the Free State of Saxony, project "BIOCOAT".

Declaration of interest

None.

References

[1] M. Zink, Biocompatibility of thin films, in: S. Nazarpour (Ed.), Thin Films Coat. Biol, Springer, Netherlands, 2013, pp. 11–67 http://link.springer.com/chapter/10.1007/978-94-007-2592-8_2, Accessed 29 August 2013.
[2] M. Golda-Cepa, A. Chorylek, P. Chytrosz, M. Brzychczy-Wloch, J. Jaworska, J. Kasperczyk, M. Hakkarainen, K. Engvall, A. Kotarba, Multifunctional PLGA/Parylene C coating for implant materials: an integral approach for biointerface optimization, ACS Appl. Mater. Interfaces 8 (2016) 22093–22105, https://doi.org/10.1021/acsami.6b08025.
[3] K. Roberts, J. Schluns, A. Walker, J.D. Jones, K.P. Quinn, J. Hestekin, J.C. Wolchok, Cell derived extracellular matrix fibers synthesized using sacrificial hollow fiber membranes, Biomed. Mater. 13 (2018)015023https://doi.org/10.1088/1748-605X/aa895c.
[4] R. Zaidel-Bar, M. Cohen, L. Addadi, B. Geiger, Hierarchical assembly of cell–matrix adhesion complexes, Biochem. Soc. Trans. 32 (2004) 416–420.
[5] R.O. Hynes, Integrins: versatility, modulation, and signaling in cell adhesion, Cell 69 (1992) 11–25, https://doi.org/10.1016/0092-8674(92)90115-S.
[6] M.A. Schwartz, M.H. Ginsberg, Networks and crosstalk: integrin signalling spreads, Nat. Cell Biol. 4 (2002) E65–E68.
[7] G. Kaushik, J. Leijten, A. Khademhosseini, Concise review: organ engineering: design, technology, and integration, Stem Cells 35 (2017) 51–60, https://doi.org/10.1002/stem.2502.
[8] L. Bedian, A.M. Villalba-Rodríguez, G. Hernández-Vargas, R. Parra-Saldivar, H.M.N. Iqbal, Bio-based materials with novel characteristics for tissue engineering applications – a review, Int. J. Biol. Macromol. 98 (2017) 837–846, https://doi.org/10.1016/j.ijbiomac.2017.02.048.
[9] M.E. Gomes, M.T. Rodrigues, R.M.A. Domingues, R.L. Reis, Tissue engineering and regenerative medicine: new trends and directions—a year in review, Tissue Eng. B Rev. 23 (2017) 211–224, https://doi.org/10.1089/ten.teb.2017.0081.
[10] L.M. Wisniewska, D.M. Dohan Ehrenfest, P. Galindo-Moreno, J.D. Segovia, F. Inchingolo, H.-L. Wang, M. Fernandes-Cruz, Molecular, Cellular and Pharmaceutical Aspects of Biomaterials in Dentistry and Oral and Maxillofacial Surgery. An Internationalization of Higher Education and Research Perspective, in: https://www.ingentaconnect.com/contentone/ben/cpb/2017/00000018/00000001/art00004, 2017Accessed 2 August 2018.
[11] D. Adamovic, B. Ristic, F. Zivic, Review of existing biomaterials—method of material selection for specific applications in orthopedics, In: Biomater. Clin. Pract, Springer, Cham, 2018, pp. 47–99, https://doi.org/10.1007/978-3-319-68025-5_3.
[12] C. Mota, M. Labardi, L. Trombi, L. Astolfi, M. D'Acunto, D. Puppi, G. Gallone, F. Chiellini, S. Berrettini, L. Bruschini, S. Danti, Design, fabrication and characterization of composite piezoelectric ultrafine fibers for cochlear stimulation, Mater. Des. 122 (2017) 206–219, https://doi.org/10.1016/j.matdes.2017.03.013.
[13] F. Shahabipour, M. Banach, T.P. Johnston, M. Pirro, A. Sahebkar, Novel approaches toward the generation of bioscaffolds as a potential therapy in cardiovascular tissue engineering, Int. J. Cardiol. 228 (2017) 319–326, https://doi.org/10.1016/j.ijcard.2016.11.210.
[14] C. Qi, J. Lin, L.-H. Fu, P. Huang, Calcium-based biomaterials for diagnosis, treatment, and theranostics, Chem. Soc. Rev. 47 (2018) 357–403, https://doi.org/10.1039/C6CS00746E.
[15] P. Mehta, R. Haj-Ahmad, M. Rasekh, M.S. Arshad, A. Smith, S.M. van der Merwe, X. Li, M.-W. Chang, Z. Ahmad, Pharmaceutical and biomaterial engineering via electrohydrodynamic atomization technologies, Drug Discov. Today 22 (2017) 157–165, https://doi.org/10.1016/j.drudis.2016.09.021.
[16] B.G. Cooper, Bordeianu, A. Nazarian, B.D. Snyder, M.W. Grinstaff, Active agents, biomaterials, and technologies to improve biolubrication and strengthen soft tissues, Biomaterials (2018) https://doi.org/10.1016/j.biomaterials.2018.07.040.
[17] F. Khan, M. Tanaka, Designing smart biomaterials for tissue engineering, Int. J. Mol. Sci. 19 (2017) 17, https://doi.org/10.3390/ijms19010017.
[18] R. Huiskes, H. Weinans, B. Van Rietbergen, The relationship between stress shielding and bone resorption around total hip stems and the effects of flexible materials, Clin. Orthop. (1992) 124–134, https://doi.org/10.1097/00003086-199201000-00014.
[19] A.C. De Luca, M. Zink, A. Weidt, S.G. Mayr, A.E. Markaki, Effect of microgrooved surface topography on osteoblast maturation and protein adsorption, J. Biomed. Mater. Res. A 103 (2015) 2689–2700, https://doi.org/10.1002/jbm.a.35407.
[20] S. Mayazur Rahman, A. Reichenbach, M. Zink, S.G. Mayr, Mechanical spectroscopy of retina explants at the protein level employing nanostructured scaffolds, Soft Matter 12 (2016) 3431–3441, https://doi.org/10.1039/C6SM00293E.
[21] M. Zink, S.G. Mayr, Ferromagnetic shape memory alloys: synthesis, characterisation and biocompatibility of Fe–Pd for mechanical coupling to cells, Mater. Sci. Technol. 30 (2014) 1579–1589, https://doi.org/10.1179/1743284714Y.0000000592.
[22] U. Allenstein, Y. Ma, a. Arabi-Hashemi, M. Zink, S.G. Mayr, Fe-Pd based ferromagnetic shape memory actuators for medical applications: biocompatibility, effect of surface roughness and protein coatings, Acta Biomater. 9 (2013) 5845–5853, https://doi.org/10.1016/j.actbio.2012.10.040.
[23] Y. Ma, M. Zink, S.G. Mayr, Biocompatibility of single crystalline Fe-Pd ferromagnetic shape memory films, Appl. Phys. Lett. 96 (2010) 213703.
[24] M. Zink, F. Szillat, U. Allenstein, S.G. Mayr, Interaction of ferromagnetic shape memory alloys and RGD peptides for mechanical coupling to cells: from ab initio calculations to cell studies, Adv. Funct. Mater. 23 (2013) 1383–1391, https://doi.org/10.1002/adfm.201201789.
[25] U. Allenstein, F. Szillat, a. Weidt, M. Zink, S.G. Mayr, Interfacing hard and living matter: plasma-assembled proteins on inorganic functional materials for enhanced coupling to cells and tissue, J. Mater. Chem. B 2 (2014) 7739–7746, https://doi.org/10.1039/C4TB01061B.
[26] U. Allenstein, S.G. Mayr, M. Zink, Contractile cell forces deform macroscopic cantilevers and quantify biomaterial performance, Soft Matter 11 (2015) 5053–5059, https://doi.org/10.1039/C5SM01212K.
[27] M. Benoit, D. Gabriel, G. Gerisch, H.E. Gaub, Discrete interactions in cell adhesion measured by single-molecule force spectroscopy, Nat. Cell Biol. 2 (2000) 313–317, https://doi.org/10.1038/35014000.
[28] U. Allenstein, E.I. Wisotzki, C. Gräfe, J.H. Clement, Y. Liu, J. Schroers, S.G. Mayr, Binary Fe-Pd submicron structures fabricated through glancing angle deposition (GLAD) for bioapplications, Mater. Des. 131 (2017) 366–374, https://doi.org/10.1016/j.matdes.2017.06.032.
[29] A. Baro, R. Reifenberger, Atomic Force Microscopy in Liquid: Biological Applications, Wiley-VCH, 2012 http://www.wiley.com/WileyCDA/WileyTitle/productCd-3527327584.html, Accessed 24 April 2017.
[30] P. Elter, T. Weihe, R. Lange, J. Gimsa, U. Beck, The influence of topographic microstructures on the initial adhesion of L929 fibroblasts studied by single-cell force spectroscopy, Eur. Biophys. J. 40 (2011) 317–327, https://doi.org/10.1007/s00249-010-0649-0.
[31] O. Thoumine, P. Kocian, A. Kottelat, J.J. Meister, Short-term binding of fibroblasts to fibronectin: optical tweezers experiments and probabilistic analysis, Eur. Biophys. J. 29 (2000) 398–408.
[32] J.-W. Tsai, B.-Y. Liao, C.-C. Huang, W.-L. Hwang, D.-W. Wang, A.E.T. Chiou, C.-H. Lin, Applications of optical tweezers and an integrated force measurement module for biomedical research, In: Proc SPIE, 2000, pp. 213–221, https://doi.org/10.1117/12.390549.
[33] N. Walter, C. Selhuber, H. Kessler, J.P. Spatz, Cellular unbinding forces of initial adhesion processes on nanopatterned surfaces probed with magnetic tweezers, Nano Lett. 6 (2006) 398–402, https://doi.org/10.1021/nl052168u.
[34] K.V. Christ, K.B. Williamson, K.S. Masters, K.T. Turner, Measurement of single-cell adhesion strength using a microfluidic assay, Biomed. Microdevices 12 (2010) 443–455, https://doi.org/10.1007/s10544-010-9401-x.
[35] E. Giacomello, J. Neumayer, A. Colombatti, R. Perris, Centrifugal assay for fluorescence-based cell adhesion adapted to the analysis of ex vivo cells and capable of determining relative binding strengths, BioTechniques 26 (1999) 758–762, (764–766).
[36] A.J. García, P. Ducheyne, D. Boettiger, Quantification of cell adhesion using a spinning disc device and application to surface-reactive materials, Biomaterials 18 (1997) 1091–1098.

[37] A.S. Goldstein, P.A. Dimilla, Application of fluid mechanic and kinetic models to characterize mammalian cell detachment in a radial-flow chamber, Biotechnol. Bioeng. 55 (1997) 616–629, https://doi.org/10.1002/(SICI)1097-0290(19970820)55:4<616::AID-BIT4>3.0.CO;2-K.
[38] A.A. Khalili, M.R. Ahmad, A review of cell adhesion studies for biomedical and biological applications, Int. J. Mol. Sci. 16 (2015) 18149–18184, https://doi.org/10.3390/ijms160818149.
[39] J.M. Sobral, V.N. Malheiro, T.W. Clyne, J. Harris, R. Rezk, W. O'Neill, A.E. Markaki, An accelerated buoyancy adhesion assay combined with 3-D morphometric analysis for assessing osteoblast adhesion on microgrooved substrata, J. Mech. Behav. Biomed. Mater. 60 (2016) 22–37, https://doi.org/10.1016/j.jmbbm.2015.12.033.
[40] A.V. Taubenberger, D.W. Hutmacher, D.J. Muller, Single-cell force spectroscopy, an emerging tool to quantify cell adhesion to biomaterials, Tissue Eng. B Rev. 20 (2014) 40–55, https://doi.org/10.1089/ten.TEB.2013.0125.
[41] J. Friedrichs, J. Helenius, D.J. Muller, Quantifying cellular adhesion to extracellular matrix components by single-cell force spectroscopy, Nat. Protoc. 5 (2010) 1353–1361, https://doi.org/10.1038/nprot.2010.89.
[42] E. Zimmerman, B. Geiger, L. Addadi, Initial stages of cell-matrix adhesion can be mediated and modulated by cell-surface hyaluronan, Biophys. J. 82 (2002) 1848–1857, https://doi.org/10.1016/S0006-3495(02)75535-5.
[43] B. Geiger, K.M. Yamada, Molecular architecture and function of matrix adhesions, Cold Spring Harb. Perspect. Biol. 3 (2011) https://doi.org/10.1101/cshperspect.a005033.
[44] B. Geiger, J.P. Spatz, A.D. Bershadsky, Environmental sensing through focal adhesions, Nat. Rev. Mol. Cell Biol. 10 (2009) 21–33, https://doi.org/10.1038/nrm2593.
[45] J.T. Parsons, A.R. Horwitz, M.A. Schwartz, Cell adhesion: integrating cytoskeletal dynamics and cellular tension, Nat. Rev. Mol. Cell Biol. 11 (2010) 633–643, https://doi.org/10.1038/nrm2957.
[46] J. Sottile, D.C. Hocking, P.J. Swiatek, Fibronectin matrix assembly enhances adhesion-dependent cell growth, J. Cell Sci. 111 (Pt 19) (1998) 2933–2943.
[47] A. Weidt, Master Thesis, Faculty of Physics and Earth Sciences, Leipzig University, (2017).
[48] P. Elter, T. Weihe, S. Bühler, J. Gimsa, U. Beck, Low fibronectin concentration overcompensates for reduced initial fibroblasts adhesion to a nanoscale topography: single-cell force spectroscopy, Colloids Surf. B: Biointerfaces 95 (2012) 82–89, https://doi.org/10.1016/j.colsurfb.2012.02.026.
[49] P. Aliuos, E. Fadeeva, M. Badar, A. Winkel, P.P. Mueller, A. Warnecke, B. Chichkov, T. Lenarz, U. Reich, G. Reuter, Evaluation of single-cell force spectroscopy and fluorescence microscopy to determine cell interactions with femtosecond-laser microstructured titanium surfaces, J. Biomed. Mater. Res. A 101A (2013) 981–990, https://doi.org/10.1002/jbm.a.34401.
[50] P. Aliuos, A. Sen, U. Reich, W. Dempwolf, A. Warnecke, C. Hadler, T. Lenarz, H. Menzel, G. Reuter, Inhibition of fibroblast adhesion by covalently immobilized protein repellent polymer coatings studied by single cell force spectroscopy, J. Biomed. Mater. Res. A 102 (2014) 117–127, https://doi.org/10.1002/jbm.a.34686.
[51] G. Wittenburg, G. Lauer, S. Oswald, D. Labudde, C.M. Franz, Nanoscale topographic changes on sterilized glass surfaces affect cell adhesion and spreading, J. Biomed. Mater. Res. A 102 (2014) 2755–2766, https://doi.org/10.1002/jbm.a.34943.
[52] I.I. Singer, S. Scott, D.W. Kawka, D.M. Kazazis, J. Gailit, E. Ruoslahti, Cell surface distribution of fibronectin and vitronectin receptors depends on substrate composition and extracellular matrix accumulation, J. Cell Biol. 106 (1988) 2171–2182, https://doi.org/10.1083/jcb.106.6.2171.
[53] T. Erdmann, U.S. Schwarz, Bistability of cell-matrix adhesions resulting from nonlinear receptor-ligand dynamics, Biophys. J. 91 (2006) L60–L62, https://doi.org/10.1529/biophysj.106.090209.
[54] B. Różycki, R. Lipowsky, T.R. Weikl, Segregation of receptor–ligand complexes in cell adhesion zones: phase diagrams and the role of thermal membrane roughness, New J. Phys. 12 (2010)095003https://doi.org/10.1088/1367-2630/12/9/095003.
[55] G. Weder, O. Guillaume-Gentil, N. Matthey, F. Montagne, H. Heinzelmann, J. Vörös, M. Liley, The quantification of single cell adhesion on functionalized surfaces for cell sheet engineering, Biomaterials 31 (2010) 6436–6443, https://doi.org/10.1016/j.biomaterials.2010.04.068.
[56] G. Weder, N. Blondiaux, M. Giazzon, N. Matthey, M. Klein, R. Pugin, H. Heinzelmann, M. Liley, Use of force spectroscopy to investigate the adhesion of living adherent cells, Langmuir ACS J. Surf. Colloids 26 (2010) 8180–8186, https://doi.org/10.1021/la904526u.